

Material reflectance retrieval in urban tree shadows with physics-based empirical atmospheric correction

Karine R. M. Adeline
 Onera
 Université de Toulouse, ISAE
 Toulouse, France
 Email: karine.adeline@onera.fr

Xavier Briottet
 Onera
 Toulouse, France

Email: xavier.briottet@onera.fr

Nicolas Paparoditis
 IGN
 Saint-Mandé, France
 Email: nicolas.paparoditis@ign.fr

Jean-Philippe Gastellu-Etchegorry
 Cesbio
 Toulouse, France
 Email: jean-philippe.gastellu-etchegorry@cesbio.cnes.fr

Abstract—Material reflectance retrieval from high spatial resolution acquisitions over urban areas requires an accurate modeling of the signal accounting for the 3D environment. Especially in tree shadows, the solar radiation incident to the ground contributing to the estimation of the reflectance has many origins linked to the plant structure and its composition. In this paper, the 3D atmospheric correction code, ICARE, limited to opaque structures like buildings, is improved thanks to an empirical correction factor taking into account the porosity of a tree crown. The validation of this method is assessed through a dataset combining a hyperspectral image and a 3D model of the scene.

to improve atmospheric correction in tree shadows applied to remote sensed images.

The goal of this paper is to enhance the performance of ICARE to estimate the part of irradiance transmitted through the crown. First, the method relies on a sensitivity analysis simulating the radiation regime at tree shadow with DART [5] through different scenario types and tree parameters. This will conduct to a physics-based empirical correction factor in the tree shadow in comparison with incident irradiance existing in shadows of opaque structure. Then, the new correction is applied on a dataset and results will be further discussed by comparing the reflectance retrieval in both sun and shadowed areas for a given ground material.

I. INTRODUCTION

With high spatial resolution imagery applied to urban areas, most of material reflectance retrieval algorithms having flat field assumptions can not compensate from the 3D environment effects like occlusions [1]. However, some radiative transfer codes [2] and adjoint radiosity methods [3] take into account the screening of the scene relief. But their main limitations are based on the fact that they often neglect either the surface multiple scatterings or the earth-atmosphere coupling whose contribution are relatively important in shadowed areas. ICARE [4] is a 3D atmospheric correction tool that is able to model all these radiative contributions and considers both slope and environment effects. In input, it requires a digital surface model (DSM). Its main drawback is that it can only consider opaque 3D structures like buildings. Such assumption does not work for single trees where part of the direct solar irradiance can be transmitted through the crown. Actually, in presence of trees, the complex interactions between the incident solar radiation and the plant materials strongly impact the radiative transfer budget received at tree shadow. Until now, many studies have assessed the contribution of both structural and biophysical tree characteristics to the top-of-canopy retrieved reflectance [3] or else the light interception beneath the tree crown [4]. However none of them have take advantage of the results of these studies

II. METHODOLOGY

A. Radiative transfer basis and empirical correction factor

The retrieval of the reflectance ρ_i for a material P in tree shadow requires the knowledge of the direct upwelling radiance R_{dir} coming from the target P and acquired by the sensor matrix pixel i , the total irradiance I_{total}^t and the upwelling direct atmospheric transmission T^\uparrow as expressed in (1). R_{dir} is deduced from the at-sensor radiance R_{sensor} , the atmospheric radiance R_{atm} which is incident to the sensor without reaching the scene and the diffuse radiance R_{env} coming from the neighbouring targets. I_{total}^t is split into the light transmitted through the tree crown I_{trans}^t , the light scattered by the atmosphere I_{diff}^t and the multiple light reflections between the scene and the atmosphere I_{coup}^t (Fig. 1).

ICARE retrieves the surface reflectance in the shadow of opaque materials by computing $I_{total_opaque}^{ICARE}$ such as in (2).

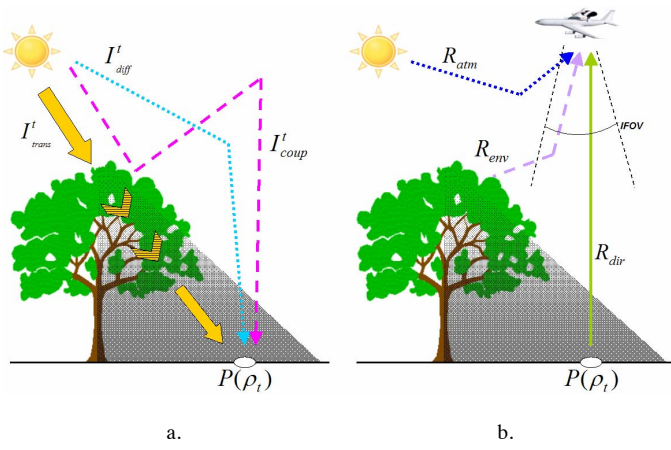


Figure 1. a. Irradiance and b. radiance components in tree shadow

$$\rho_t(P) = \frac{R_{dir}(i)}{I_{total}^i(P)} \cdot \pi \cdot T^\uparrow \quad (1)$$

$$\text{with } \begin{cases} R_{sensor}(i) = R_{dir}(i) + R_{env}(i) + R_{atm}(i) \\ I_{total}^i(P) = I_{trans}^i(P) + I_{diff}^i(P) + I_{coup}^i(P) \end{cases}$$

$$I_{total_opaque}^{ICARE} = I_{diff}^{ICARE} + I_{coup}^{ICARE} \quad (2)$$

In order to compensate the error of neglecting the radiative term I_{trans}^i in ICARE modeling for tree shadows, the method is to apply an empirical correction factor β on the ICARE retrieved reflectance thanks to some prior knowledge of the tree properties. As such, β is deduced from the direct simulations of the radiation regime at shadow in presence of a single tree with DART. Two scenario types are generated (3): the first with a semi-transparent tree crown (I_{total}^{DART}) and the second with a tree crown that is assumed to be fully opaque ($I_{total_opaque}^{DART}$).

$$\begin{aligned} I_{total}^{DART} &= I_{trans}^{DART} + I_{diff}^{DART} + I_{coup}^{DART} \\ I_{total_opaque}^{DART} &= I_{diff}^{DART} + I_{coup}^{DART} \end{aligned} \quad (3)$$

Then β is defined as the ratio between the transmitted and the total irradiance received at tree shadow. Finally, new material reflectances $\rho^{ICARE,J}$ are computed for tree shadows from total original ICARE reflectances ρ^{ICARE} (4).

$$\begin{aligned} I_{total}^i &\approx \left[I_{total_opaque}^{ICARE} + I_{total_opaque}^{ICARE} \cdot \left(\frac{I_{trans}^{DART}}{I_{total_opaque}^{DART}} \right) \right] = I_{total_opaque}^{ICARE} \cdot (1 + \beta) \\ \Rightarrow \rho^{ICARE,J} &= \frac{\rho^{ICARE}}{1 + \beta} \end{aligned} \quad (4)$$

B. Simulations of the radiative budget at tree shadow and sensitivity analysis of the tree parameters

The scene represents a single tree that casts a shadow at ground and is assumed to have an ellipsoidal shape. The branches of the tree are not taken into account in this study. The full description of the scene and the tree parameterization

TABLE I. DART INPUT PARAMETERS

Scene and atmosphere description	Unit	Values
Scene ground size	m ²	23*23
Cell size	m ³	0.4*0.4*0.4
Sun zenith and azimuth angles	degree	46; 90 (clockwise)
Aerosol model and visibility	-	Urban model with 23km

Tree description	Unit	Values
Tree height	m	14.2
Crown height and diameter	m	9.4; 6
Trunk height (below and inside crown) and diameter	m	4.8; 7.2; 0.4
Tree LAI (8 cases)	m ² .m ⁻²	1-2-3-4-5-6-7-8
LAD (3 cases)	-	Spherical (ALA ^a = 57°) and ellipsoidal (ALA ^a = 10° and 80°)
gap fraction as randomly distributed holes (3 cases)	%	0-30-70

a. Average Leaf Angle

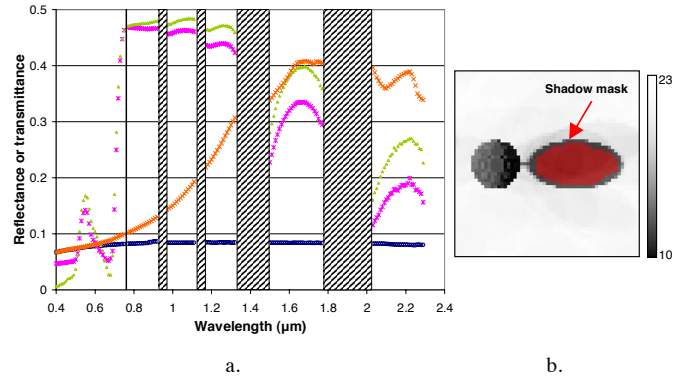


Figure 2. a. Graph of the reflectance (magenta) and transmittance (green) of leaves from a quercus palustris in ANGERS93 [7], the reflectance of the trunk (orange) and asphalt at ground (blue) from DART, striped bands stand for atmospheric windows; b. At-sensor radiance image of the scene expressed in $W.m^{-2}.sr^{-1}.\mu m^{-1}$ at 550nm for the opaque tree scenario

is detailed in Table I. The simulations are run over the reflective domain $0.4-2.3\mu m$ in 138 spectral bands. The optical properties of the leaves, the trunk of the tree and the ground material are plotted in Fig. 2.a. For the two scenario types, the total irradiance computed at ground is a mean over a mask lying in the tree shadow as illustrated in Fig. 2.b.

Since the downwelling irradiance at shadow depends on the tree architecture and its composition, a sensitivity analysis is carried out through three variable parameters of the tree: the LAI, the LAD and the crown gap fraction. These latter are often mentioned to be the primary sources of light interception within the crown [3][4][8]. Their relative contribution to the variability of I_{total}^{DART} in the shadows will be compared to $I_{total_opaque}^{DART}$ following the work of [9]. Through this analysis, the importance of the correction factor β will be evaluated.

III. DATASET AND PREPROCESSING STEPS

A dataset including VHR hyperspectral images and LIDAR data has been acquired over the city of Norrköping, Sweden, on September 2nd 2009 between 8:00 and 8:30 UTC. The push-broom sensor Itres CASI 1500 collected 24 spectral bands from 381.9nm to 1040.4nm at a spatial resolution of 0.5m. A Digital surface model (DSM) with 0.25 m resolution was built from LIDAR sensor Optech ALTM Gemini. The study area is typical of a European urban landscape mainly composed of buildings, roads and green areas [10]. Since the image data was not calibrated and no information about atmospheric conditions, ground truth measurements or inlab calibration was available, a rough calibration was applied with the help of 6S [1][11]. Finally, 14 spectral bands over 24 for the hyperspectral image were selected out of the atmospheric absorption windows. An extraction of the image has shown good results for classification purposes with ICARE in tree shadows but has still some discrepancies in the retrieved ground reflectance [1].

IV. RESULTS

LAI, LAD and gap fraction are geometric factors of the tree architecture. As such, their respective mean contribution relative to each other to I_{total}^{DART} in tree shadow is little wavelength-dependent. Each one has a standard deviation of less than 0.5% over the whole reflective domain. The results show that LAI has a mean contribution value of 44% which is about twice that of the others (LAD: 28% and gap fraction: 28%). Consequently, a first approach for an empiric correction could be only to consider the major influence attributed to the LAI and neglect the others by attributing fixed values to them. Further, LAD will be set to have a spherical distribution, which is an assumption mainly done in the literature. And the gap fraction will be fixed to 0% since on a closer examination of the airborne extracted image, the tree shadows seem to be homogeneously dark (Fig. 5.a).

Afterwards, the factor β is computed in relationship with the LAI value and the wavelength in Fig. 3.a. As expected, the lower the LAI is, the higher the sunlight penetrates the tree crown and the higher β is sensitive. Also the relative importance of the I'_{trans} modeling is highlighted for the long wavelengths where the total amount of signal at shadow drastically decreases. For high LAI, I_{trans} is smaller and is almost entirely composed of the multiple scatterings inside the crown. This explains the change of slope around the red-edge between 650nm and 750nm in Fig. 3.b.

The LAI of a single tree is often estimated from the computation of the NDVI above the tree crown in the image with the red and near-infrared spectral bands, here respectively 668nm and 754nm [12]. NDVI-LAI relationship is well-known to fit to an exponential model which reaches a saturation threshold for high NDVI depending on many parameters: the sensor type, the spatial resolution, the tree species, etc. [13]. In the paper, the results of only one tree will be presented. This tree is encircled in red in the airborne image in Fig. 5.a. It has a mean NDVI of 0.75 for the image data expressed in radiances and 0.8 with reflectances from ICARE outputs. These NDVI values are usually located to the saturation level for high LAI.

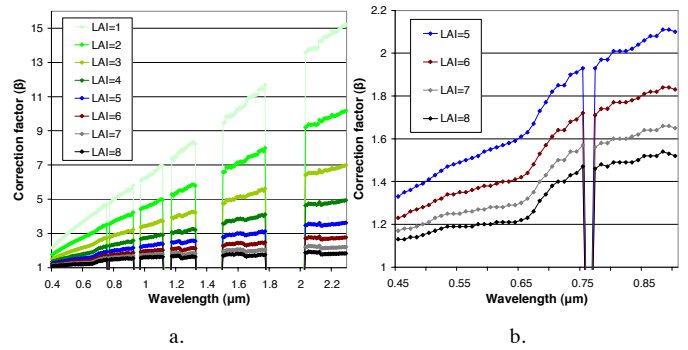


Figure 3. a. Graph of the correction factor in function of the LAI values over the reflective domain; b. Same plot as previously for high LAI values over the spectral range corresponding to that of the hyperspectral airborne image

If it reveals to be the case, the choice of a high LAI firstly agrees with the good performances of ICARE by considering that the trees behave like opaque materials. In [1], ICARE classification results in tree shadows were about 70%. Furthermore, it is to be noticed that the graph of I_{total}^{DART} received in shade against $I_{total_opaque}^{DART}$ shows that the error in the choice of LAI is minimized when the LAI is high. Then, LAI will be arbitrary set to 8.

Thereafter, the correction factor β is only applied for the tree shadow in the image over three materials: road asphalt, grass and bicycle path asphalt. The resulting reflectance image is shown in Fig. 5.b. The comparison of spectra retrieved in the sun and shade in Fig. 5.c. is assessed through the computation of the R^2 and the RMSE in Table II. Finally, the new empirical atmospheric correction makes smoother the flat spectrum of road and bicycle path asphalt with similar R^2 . The most obvious improvements in terms of RMSE are shown for the bicycle path which is closer to the tree and so more influenced to its radiative impact. For grass, ICARE results are better but the standard deviation of the values is high in NIR. Actually, the accuracy of ICARE retrieved reflectance with ground truth measurements is about 0.04.

V. CONCLUSION AND OUTLOOK

For trees with high LAI, 3D atmospheric correction considering opaque materials with ICARE has showed good performances in the shadow. However, improvements can be done to compensate for the part of the transmitted light interacting with plant materials especially for NIR-SWIR spectral bands. The empirical correction factor presented in this paper helps to understand the physics of the radiation regime beneath the tree crown. These first results are promising. Nevertheless, they could drastically depend on the choice of the tree characterization: leaf spectra, LAI, LAD and gap fraction etc. Others reasons may also affect the results such as the accuracy of the rough calibration applied to the data, the relevance of the sensitivity analysis with the number of values taken for each variable parameter, the choice of the LAI depending to the NDVI-LAI relationship, etc. The ongoing works are directed to the improvement of the physics-based correction with a more complete sensitivity analysis including more parameters (optical properties of plant tissues, branches).

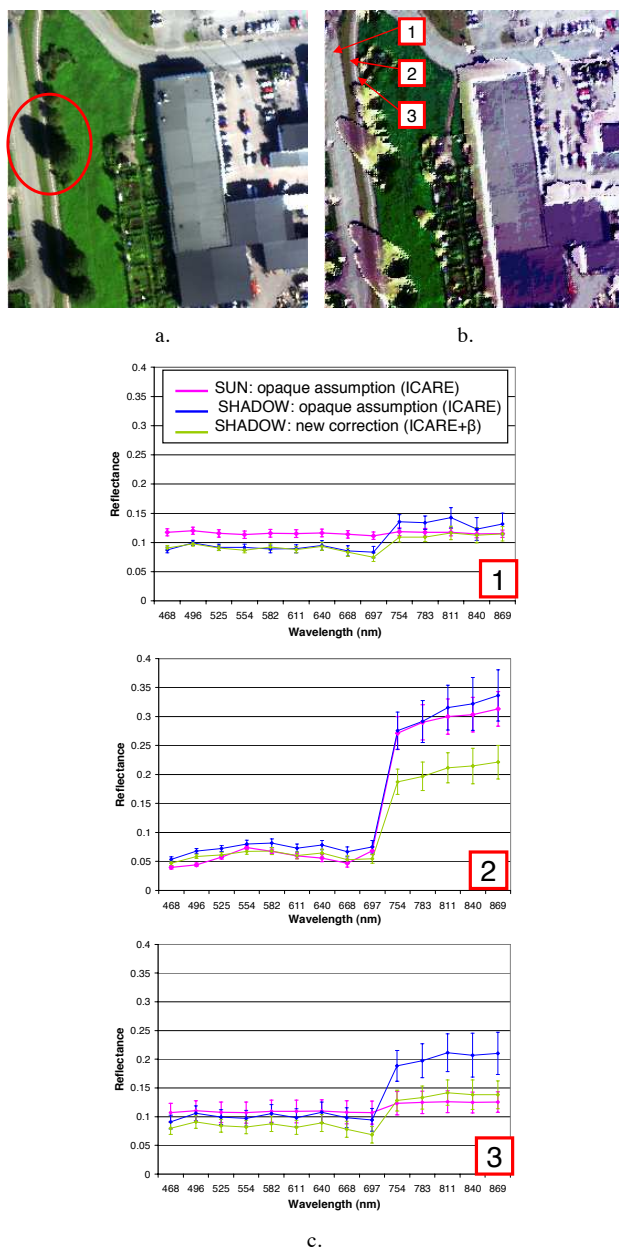


Figure 4. a. The at-sensor image; b. Reflectance image with the empirical atmospheric correction; c. Plots of the material reflectance in sun and shade for the road (1), the grass (2) and the bicycle path (3)

TABLE II. ASSESSMENT OF THE NEW EMPIRICAL CORRECTION WITH MEAN ACCURACY MEASURES OVER THE TREE SHADOW

Accuracy measures	Atmospheric correction	Ground material at tree shadow		
		ROAD	GRASS	BICYCLE PATH
R ²	ICARE (opaque assumption)	17.12%	99.64%	99.30%
	ICARE+β (empirical correction)	26.16%	99.52%	98.19%
RMSE	ICARE (opaque assumption)	2.30%	1.58%	4.74%
	ICARE+β (empirical correction)	2.22%	5.37%	2.23%

Finally, this new method must be validated over other datasets. To this end, a new experiment has been done in October, 2012 with our HYSPEX hyperspectral cameras with an extensive ground truth allowing a better validation.

ACKNOWLEDGMENT

We would like to thank Gustav Tolt from Sweden Defense Research Agency (FOI) for providing the dataset, HPC-SA for the raytracer Raybooster (<http://www.hpc-sa.com>) in ICARE and Cesbio for the DART tool. This work is funded by the ANR VegDUD project.

REFERENCES

- [1] K.R.M. Adeline, X. Briottet and N. Paparoditis, "Material reflectance retrieval in shadow due to urban vegetation from 3D lidar data and hyperspectral airborne imagery", In: Proceedings of 32nd EARSeL Symposium, Advances in Geosciences, Mykonos, Greece, May 2012.
- [2] R. Richter and D. Schlöpfer, "Atmospheric / Topographic Correction for Satellite Imagery", DLR report DLR-IB 565-02/11, Wessling, Germany, 2011, pp. 202.
- [3] C. Borel, K. Ewald, M. Manzano, C. Wamsley and J. Jacobson, "Adjoint Radiosity Based Algorithms For Retrieving Target Reflectances In Urban Area Shadows", In: Proceedings of 6th EARSeL SIG IS workshop, Tel Aviv University, 16-19 March 2009.
- [4] G. P. Asner, "Biophysical and biochemical sources of variability in canopy reflectance", Remote Sensing of Environment, Vol. 64, 1998, pp. 234-253.
- [5] F. de Castro and N. Fetcher, "Three dimensional model of the interception of light by a canopy", Agricultural and Forest Meteorology, Vol. 90, 1998, pp. 215-233.
- [6] S. Lachérade, C. Miesch, D. Boldo, X. Briottet, C. Valorge and H. Le Men, "ICARE: A physically-based model to correct atmospheric and geometric effects from high spatial and spectral remote sensing images over 3D urban areas", Meteorology and Atmospheric Physics Publisher Springer Wien, Special Issue on CAPITOU Experiment (Special Editors: L. Gimeno, V. Masson and A. J. Arnfield), Vol. 102, No. 3-4, 2008, pp. 209-222.
- [7] J.-P. Gastellu-Etchegorry, V. Demarez, V. Pinel and F. Zagolski, "Modeling Radiative Transfer in Heterogeneous 3-D Vegetation Canopies", Remote Sensing of Environment, Vol.58, 1996, pp. 131-156.
- [8] B. Hosgood, S. Jacquemoud, G. Andreoli, J. Verdebout, G. Pedrini, and G. Schmuck, "Leaf Optical Properties EXperiment 93 (LOPEX93)", European Commission – Joint Research Centre, Ispra (Italy), EUR 16095 EN, 1994, pp. 20.
- [9] D.A. Sampson and F.W. Smith, "Influence of canopy architecture on light penetration in lodgepole pine (Pinus contorta var. latifolia) forests", Agricultural and Forest Meteorology, Vol. 64, 1993, pp. 63-79.
- [10] C. Bacour, S. Jacquemoud, Y. Tourbier, M. Dechambre and J.-P. Frangi, "Design and analysis of numerical experiments to compare four canopy flextance models". Remote Sensing of Environment, Vol. 79, 2002, pp. 72-83.
- [11] G. Tolt, M. Shimoni and J. Ahlberg, "A shadow detection method for remote sensing images using VHR hyperspectral and LIDAR data", In: Proceedings of IGARSS, Vancouver Canada, 25-29 July 2011.
- [12] E. Vermote, D.Tanré, J.L. Deuze, M.Herman and J.J. Morcrette, "Second simulation of the satellite signal in the solar spectrum: an overview", IEEE Trans. Geosci. Remote Sens., 1996.
- [13] J.W. Rouse, R.H. Haas, J.A. Schell, D.W. Deering and J.C. Harlan, "Monitoring the Vernal Advancements and Retrogradation (Greenwave Effect) of Nature Vegetation", NASA/GSFC Type-III Final Report, Greenbelt, MD, USA, 1974, pp. 164.
- [14] K. Soudani, C. François, G. le Maire, V. le Dantec and E. Dufrêne, "Comparative analysis of IKONOS, SPOT, and ETM+ data for leaf area index estimation in temperate coniferous and deciduous forest stands", Remote Sensing of Environment, Vol. 102, 2006, pp. 161-175.

